On Self-excited Auto-parametric Systems

Abadi
Department of Mathematics
University of Utrecht
PO Box 80.010, 3508 TA Utrecht
The Netherlands

Abstract

We consider a Rayleigh type of self-excited auto-parametric system. We study the semi-trivial solution and its domain of instability where non-trivial solutions are initiated. We are interested in the existence and stability of the non-trivial solutions and we analyze the behaviour of the solutions by examining it for various values of some parameters. We divide the discussion on the non-trivial solution in exact resonance and near resonance cases. In the analysis we use both normal forms (or averaging) and numerical bifurcation path-following techniques. The system displays a rich pattern of different bifurcations, a robust heteroclinic cycle and instability behaviour.

Key words. Auto-parametric, self-excited, stability, bifurcation.

1 Introduction

An autoparametric system is a vibrating system which consists of at least two subsystems; an Oscillator which generally be in a vibrating state and the Excited System which is excited indirectly and is coupled to the Oscillator in a nonlinear way such that the Excited System can be at rest while the Oscillator is vibrating (this state is called *semi-trivial solution*).

A self-excited auto-parametric system is a special type of auto-parametric system with a self-excited oscillator in its vibrating state. There are many

mechanical systems which are considered to have the characteristics of self-excited auto-parametric systems, for instance systems with flow-induced vibrations; see for instance the books by Tondl, Nabergoj, Verhulst, and Ruijgrok ([7], [12], or [13]) and other references there. For a discussion of the applications in mechanics, the reader may refer to [8], [11], or [13].

This paper discusses a Rayleigh type self-excited auto-parametric system. We study the solutions of the system, semi-trivial and non-trivial solutions, and analyze their behaviour. By using the response-oriented approach we study the instability domain of the solutions. And we focus on varying the damping coefficient κ of the excited system (and fixing the other parameters) to see the behaviour of the solutions (stabilities and bifurcations). See the monographs by Guckenheimer and Holmes [2] or Wiggins [15] for the references on the bifurcation theory.

2 Formulation of a Rayleigh type self-excited auto-parametric system

We consider a self-excited auto-parametric system of Rayleigh type in the non-dimensional form:

$$\begin{aligned} x'' - \beta(1 - x'^2)x' + x + \gamma_1 y^2 &= 0 \\ y'' + \kappa y' + q^2 y + \gamma_2 xy &= 0. \end{aligned} \tag{2.1}$$

where $\beta > 0,$ is the self-excitation coefficient, $\kappa > 0$ is the damping coefficient of the Excited System, γ_1 and γ_2 are the nonlinear coupling coefficients; q is the tuning coefficient expressing the ratio of natural frequencies of the undamped linearized subsystems, where the frequency of the x-mode is normalized to 1. We restrict our discussion in this paper by considering the important resonance $q = \frac{1}{2}$ and nearby (detuned) values. The prime indicates the derivative with respect to the non-dimensional time variable. The first equation of (2.1) refers to the motion of the oscillator whereas the second one refers to the excited subsystem. We have chosen nonlinear coupling terms which are important in this particular resonance case; see also the discussion at the end of this paper.

To study the system above we divide our discussion into two parts. That is, the semi-trivial solution and the non-trivial solution.

First, we assume that all the parameters in system (2.1) are small and in

order to apply the averaging method (see [9]), we rescale the parameters as follows. Let $\beta = \epsilon\bar{\beta}$, $\kappa = \epsilon\bar{\kappa}$, $\gamma_1 = \epsilon\bar{\gamma}_1$, $\gamma_2 = \epsilon\bar{\gamma}_2$, and take $q^2 = \frac{1}{4} + \epsilon\sigma$. Then, substituting these into equation (2.1), after dropping the bars, we have the following standard form

$$\begin{aligned} x'' + x &= \epsilon(\beta(1 - x'^2)x' - \gamma_1 y^2) \\ y'' + \frac{1}{4}y &= -\epsilon(\kappa y' + \sigma y + \gamma_2 xy). \end{aligned} \tag{2.2}$$

Further analysis of system (2.2), as we shall see in the subsequent section, leads us to the conclusion that periodic solutions exist.

3 The semi-trivial solution and its stability

The semi-trivial solution is defined as the solution of the system (2.2) by putting $y = 0$. Thus, we have the well-known Rayleigh equation

$$x'' + x = \epsilon\beta(1 - x'^2)x', \ y = 0. \tag{3.1}$$

We put $x(\tau) = R\cos(\tau + \psi)$ with $x'(\tau) = -R\sin(\tau + \psi)$ to obtain slowly varying equations for R and ψ; after averaging over τ, we obtain:

$$\begin{aligned} R' &= \epsilon\frac{1}{2}\beta R(1 - \frac{3}{4}R^2) \\ \psi' &= 0. \end{aligned} \tag{3.2}$$

For this standard procedure in averaging theory see [9] or [14]. Finding the non-trivial equilibrium for R, we have $R = R_0 = \sqrt{\frac{4}{3}}$. And, because of the translation property for autonomous systems we may take $\psi = \psi_0 = 0$. Therefore, $x_0(\tau) = R_0\cos(\tau + \psi_0) = \sqrt{\frac{4}{3}}\cos\tau$ is an approximation to the periodic solution of (3.1) up to $\mathcal{O}(\epsilon)$. By a simple calculation we conclude that the semi-trivial solution is a periodic stable solution with period near to 2π (stable in equation (3.1)).

For the stability investigation of the semi-trivial solution $x_0(\tau)$ in the full system (2.2), we apply a small perturbation to the solution, i.e., we consider the perturbations:

$$x = x_0(\tau) + u, \text{ and } y = 0 + v. \tag{3.3}$$

Then, we substitute (3.3) into system (2.2). Thus, after performing linearization, we obtain the following uncoupled equations.

$$\begin{aligned} u'' + u &= \epsilon\beta(1 - 3x_0'(\tau)^2)u', \\ v'' + \frac{1}{4}v &= -\epsilon(\kappa v' + \sigma v + \gamma_2 x_0(\tau)v). \end{aligned} \tag{3.4}$$

By the averaging method (putting $u(\tau) = r\cos(\tau+\varphi)$, $u'(\tau) = -r\sin(\tau+\varphi)$ for the first equation of (3.4)), we can show that the differential equation for r gives asymptotic stability of the trivial solution $u = 0$. Thus, the semi-trivial solution is stable in the x-direction. Therefore it remains to analyze the second equation of (3.4) in order to investigate the stability of the semi-trivial solution in the full system.

The second equation of (3.4) is of Mathieu type and its main instability domain is found for values of q near $\frac{1}{2}$. (See [14] Appendix 2, for a description of the Mathieu type equation). Then, the solution of the equation can be analyzed by putting

$$v(\tau) = R\cos(\frac{1}{2}\tau + \psi), \text{with } v'(\tau) = -\frac{1}{2}R\sin(\frac{1}{2}\tau + \psi). \tag{3.5}$$

By substituting the relations in (3.5) into equation (3.4) for v, then applying the averaging over τ and after absorbing the rescaling factor ϵ into τ, we obtain:

$$\begin{aligned} R' &= -\frac{1}{4}\kappa R + \frac{1}{4}R\gamma_2 R_0 \sin 2\psi, \\ \psi' &= \frac{1}{2}\sigma + \frac{1}{4}\gamma_2 R_0 \cos 2\psi, \end{aligned} \tag{3.6}$$

where R_0 is the amplitude of the semi-trivial solution we obtained earlier.

From the right-hand sides of (3.6), we can eliminate the variable ψ and after applying the response-oriented approach (see [12] or [13]), we have the following relation for the boundary of the stability domain:

$$R_c^2 = R_0^2 = \frac{1}{\gamma_2^2}(\kappa^2 + 4\sigma^2), \tag{3.7}$$

where R_c stands for R-critical. Thus, for $q^2 = \frac{1}{4} + \epsilon\sigma$, we have the stability boundary values in terms of q and κ as follows:

$$q^2 = \frac{1}{4} + \epsilon\sqrt{\frac{\gamma_2^2 R_0^2 - \kappa^2}{4}}, \tag{3.8}$$

which exists for $\kappa \leq \gamma_2\sqrt{\frac{4}{3}}$. As an illustration, we take $\gamma_2 = 2,\ \kappa = 1$, and we have a stability boundary curve, as shown by the R_c-curve in figure 1 below.

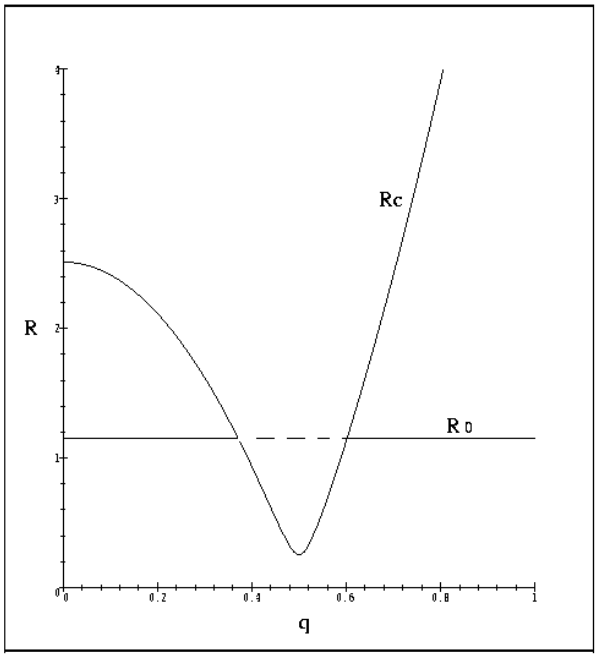

Figure 1: R_0 corresponds to the semi-trivial solution and R_c corresponds to the stability boundary curve as a function of tuning ratio q for $\gamma_2 = 2,\ \kappa = 1, \epsilon = 0.1$. Values of $R_0 > R_c$ correspond with instability.

The value $\kappa = \gamma_2\sqrt{\frac{4}{3}}$ is a *bifurcation value* where the semi-trivial solution changes its property and a non-trivial solution is initiated. We will see this phenomenon in the subsequent section.

4 Analysis of non-trivial solutions

The non-trivial solutions of (2.2) can be written in the following form:

$$x = R_1\cos(\tau + \psi_1) \text{ and } y = R_2\cos(\frac{1}{2}\tau + \psi_2). \tag{4.1}$$

We substitute (4.1) into (2.2), then we apply the averaging method. Thus, we obtain the following averaged system (after absorbing the rescaling factor

ϵ into τ).

$$\begin{aligned} R_1' &= \frac{1}{2}\beta R_1 - \frac{3}{8}\beta R_1^3 + \frac{1}{4}\gamma_1 R_2^2 \sin(\psi_1 - 2\psi_2) \\ \psi_1' &= \frac{1}{4}\gamma_1 \frac{R_2^2}{R_1}\cos(\psi_1 - 2\psi_2) \\ R_2' &= -\frac{1}{2}\kappa R_2 - \frac{1}{2}\gamma_2 R_1 R_2 \sin(\psi_1 - 2\psi_2) \\ \psi_2' &= \sigma + \frac{1}{2}\gamma_2 R_1 \cos(\psi_1 - 2\psi_2). \end{aligned} \tag{4.2}$$

Note that the combination angle $\phi = \psi_1 - 2\psi_2$ figures in system (4.2) and we may reduce the system to:

$$\begin{aligned} R_1' &= \frac{1}{2}\beta R_1 - \frac{3}{8}\beta R_1^3 + \frac{1}{4}\gamma_1 R_2^2 \sin\phi \\ R_2' &= -\frac{1}{2}\kappa R_2 - \frac{1}{2}\gamma_2 R_1 R_2 \sin\phi \\ \phi' &= -2\sigma + (\frac{1}{4}\gamma_1 \frac{R_2^2}{R_1} - \gamma_2 R_1)\cos\phi. \end{aligned} \tag{4.3}$$

To remove the singularity of the vector field in system (4.3) we define

$$\rho = R_2^2,\ u = R_1 \cos\phi,\ v = R_1 \sin\phi, \tag{4.4}$$

and the transformed system reads

$$\begin{aligned} \rho' &= -\kappa\rho - \gamma_2 \rho v \\ u' &= \frac{1}{2}\beta(1 - \frac{3}{4}R_1^2)u + \gamma_2 uv + 2\sigma v \\ v' &= \frac{1}{2}\beta(1 - \frac{3}{4}R_1^2)v + \frac{1}{4}\gamma_1\rho - \gamma_2 u^2 - 2\sigma u, \end{aligned} \tag{4.5}$$

where $R_1^2 = u^2 + v^2$.

To study system (4.5), we consider exact resonance ($\sigma = 0$), which is simpler, and near-resonance ($\sigma \neq 0$).

The fixed points of system (4.5) correspond to periodic solutions of system (4.2). First, we find the fixed points by assuming that ρ, u, and v are constants. Then by fixing the values of the parameters β, γ_1, and γ_2 and letting the value of κ varies we study the bifurcations of the fixed points.

5 Exact resonance

Putting $\sigma = 0$ and assuming that $\beta > 0,\ \gamma_1 > 0,$ and $\gamma_2 > 0$, system (4.5) becomes

$$\begin{aligned} \rho' &= -\kappa\rho - \gamma_2\rho v \\ u' &= \frac{1}{2}\beta(1 - \frac{3}{4}(u^2+v^2))u + \gamma_2 uv \\ v' &= \frac{1}{2}\beta(1 - \frac{3}{4}(u^2+v^2))v + \frac{1}{4}\gamma_1\rho - \gamma_2 u^2. \end{aligned} \tag{5.1}$$

Note that system (5.1) is invariant under $(\rho, u, v) \to (\rho, -u, v)$. $\rho = 0$ is an invariant manifold of the system. This is obvious since taking $\rho = 0$ is related to our previous analysis of the semi-trivial solution. In addition, $u = 0$ is also an invariant manifold of system (5.1).

5.1 Fixed points and their bifurcations

To analyze the fixed points of system (5.1), we will make use the existence of the invariant manifolds $\rho = 0$ and $u = 0$.

Solving $f_1(\rho, u, v) = 0, f_2(\rho, u, v) = 0, f_3(\rho, u, v) = 0$, where $f_1,\ f_2,\ f_3$ are the right hand sides of (5.1), we obtain the following fixed points. $\mathbf{x_{00}} = (\rho_0, u_0, v_0) = (0, 0, 0)$ (the trivial solution), $\mathbf{x_{10}} = (0, 0, \sqrt{\frac{4}{3}})$, and $\mathbf{x_{20}} = (0, 0, -\sqrt{\frac{4}{3}})$ (the semi-trivial solution) and the following fixed points corresponding with non-trivial periodic solutions

$$\mathbf{X_1} = \left(\frac{2\beta\kappa}{\gamma_1\gamma_2}(1 - \frac{3}{4}\frac{\kappa^2}{\gamma_2^2}), 0, -\frac{\kappa}{\gamma_2}\right), \tag{5.2}$$

and

$$\mathbf{X_2} = \left(\frac{16}{3}\frac{\gamma_2}{\gamma_1}(1 - 2\frac{\kappa}{\beta}), \pm\sqrt{\frac{4}{3}(1 - \frac{3}{4}\frac{\kappa^2}{\gamma_2^2}) - \frac{8}{3}\frac{\kappa}{\beta}}, -\frac{\kappa}{\gamma_2}\right). \tag{5.3}$$

Note that the points $\mathbf{x_{00}},\ \mathbf{x_{10}}$, and $\mathbf{x_{20}}$ are in the invariant manifold $\rho = 0$, the points $\mathbf{x_{00}},\ \mathbf{x_{10}},\ \mathbf{x_{20}}$ and $\mathbf{X_1}$ are in the invariant manifold $u = 0$. Thus, we may begin the analysis of the fixed points from the manifolds where they are in, while we need to analyze the point $\mathbf{X_2}$ separately.

We apply linear analysis by, first, finding the Jacobian matrix of system (5.1). Then we find the eigenvalues of the corresponding fixed points whose

stability properties are to be determined. The Jacobian matrix of system (5.1) is as follows.

$$J = \begin{pmatrix} -\kappa - \gamma_2 v & 0 & -\gamma_2 r \\ 0 & \frac{1}{2}\beta - \frac{9}{8}\beta u^2 - \frac{3}{8}\beta v^2 + \gamma_2 v & -\frac{3}{4}\beta uv + \gamma_2 u \\ \frac{1}{4}\gamma_1 & -\frac{3}{4}\beta uv - 2\gamma_2 u & \frac{1}{2}\beta - \frac{3}{8}\beta u^2 - \frac{9}{8}\beta v^2 \end{pmatrix} \quad (5.4)$$

In the invariant manifold $\rho = 0$, where the points $\mathbf{x_{00}}$, $\mathbf{x_{10}}$, and $\mathbf{x_{20}}$ are located, the corresponding 2×2 Jacobian matrix is as follows.

$$J_1 = \begin{pmatrix} \frac{1}{2}\beta - \frac{9}{8}\beta u^2 - \frac{3}{8}\beta v^2 + \gamma_2 v & -\frac{3}{4}\beta uv + \gamma_2 u \\ -\frac{3}{4}\beta uv - 2\gamma_2 u & \frac{1}{2}\beta - \frac{3}{8}\beta u^2 - \frac{9}{8}\beta v^2 \end{pmatrix} \quad (5.5)$$

Linear analysis yields that $(0,0)$ which has eigenvalues $\lambda_1 = \lambda_2 = \frac{1}{2}\beta$ is an unstable node with straight lines phase flows pointing outward. In $(0, \sqrt{\frac{4}{3}})$ the eigenvalues are $\gamma_2\sqrt{\frac{4}{3}}$ and $-\beta$. This corresponds with a saddle point with its stable manifold on the v axis. In $(0, -\sqrt{\frac{4}{3}})$ the eigenvalues are $-\gamma_2\sqrt{\frac{4}{3}}$ and $-\beta$. This corresponds with a stable node with parabolic phase curves pointing inward. By some algebraic manipulation on the equations in (5.1) for $\rho = 0$ we obtain a separatrix curve $u^2 + v^2 = \frac{4}{3}$ connecting the points $(0, \sqrt{\frac{4}{3}})$ and $(0, -\sqrt{\frac{4}{3}})$; An orbit which starts from a point outside the curve will never cross the separatrix curve and it will go either to the stable manifold of $(0, \sqrt{\frac{4}{3}})$ or to the stable manifold of $(0, -\sqrt{\frac{4}{3}})$. Some authors call such a separatrix curve a *saddle-sink connection*. This saddle-sink connection actually corresponds with the semi-trivial solution obtained previously as we can check it by using transformation (4.4). For the illustration of the dynamics on the $u-v$ plane see Figure 2.

In the invariant manifold $u = 0$, where the points $\mathbf{x_{00}}$, $\mathbf{x_{10}}$, $\mathbf{x_{20}}$, and $\mathbf{X_1}$ are located, the corresponding 2×2 Jacobian matrix is as follows.

$$J_2 = \begin{pmatrix} -\kappa - \gamma_2 v & -\gamma_2 r \\ \frac{1}{4}\gamma_1 & \frac{1}{2}\beta - \frac{3}{8}\beta u^2 - \frac{9}{8}\beta v^2 \end{pmatrix} \quad (5.6)$$

Using a similar analysis as above, we find that in $(0,0)$ the eigenvalues are $-\kappa$ and $\frac{1}{2}\beta$. This corresponds with a saddle point with its unstable manifold on the v axis. In $(0, \sqrt{\frac{4}{3}})$ the eigenvalues are $-\kappa - \gamma_2\sqrt{\frac{4}{3}}$ and $-\beta$ which correspond with a stable node. An interesting phenomenon happens at $(0, -\sqrt{\frac{4}{3}})$. The eigenvalues are $-\kappa + \gamma_2\sqrt{\frac{4}{3}}$ and $-\beta$, as can be seen from the following matrix

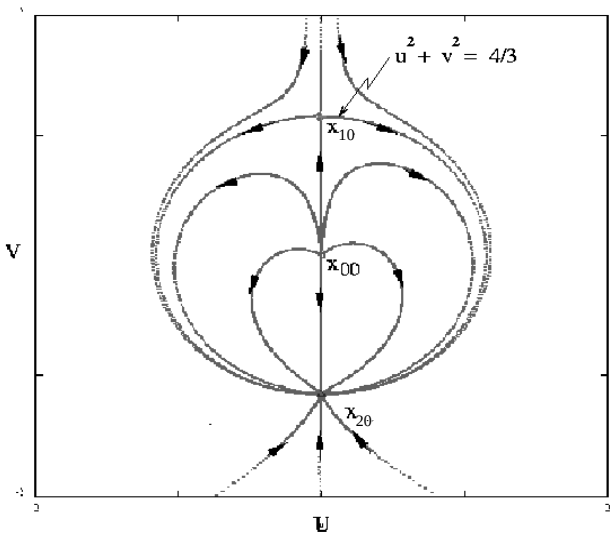

Figure 2: The dynamics in the $u-v$ plane.

which is obtained by substituting $(0, -\sqrt{\frac{4}{3}})$ into J_2.

$$J_p = \begin{pmatrix} -\kappa + \gamma_2\sqrt{\frac{4}{3}} & 0 \\ \frac{1}{4}\gamma_1 & -\beta \end{pmatrix} \tag{5.7}$$

Focusing on the change of values of the parameter κ, we see that $\kappa = \gamma_2\sqrt{\frac{4}{3}}$ is a critical value where the corresponding fixed point changes its property (recall the bifurcation value we mentioned in Section 3). We can check easily that $\kappa > \gamma_2\sqrt{\frac{4}{3}}$ results in the point $(0, -\sqrt{\frac{4}{3}})$ to be a stable node, while $\kappa < \gamma_2\sqrt{\frac{4}{3}}$ results in the point $(0, -\sqrt{\frac{4}{3}})$ to be a saddle. To see what happens at $\kappa = \gamma_2\sqrt{\frac{4}{3}}$ we apply the center manifold approach (see [1] for details).

We consider the equations (5.1)(i) and (5.1)(iii) for ρ and v, respectively, by taking $u = 0$. For the sake of simplicity, we fix the values of $\beta = 2,\ \gamma_1 = 1,\ \gamma_2 = 2$. Thus, the system we consider is as follows.

$$\begin{aligned} \rho' &= -\kappa\rho - 2\rho v \\ v' &= v - \frac{3}{4}v^3 + \frac{1}{4}\rho. \end{aligned} \tag{5.8}$$

We translate the point $(0, -\sqrt{\frac{4}{3}})$ to (0,0), the bifurcation value to 0, and take $h(\bar{\rho}, \bar{\kappa}) = a_1\bar{\rho}^2 + a_2\bar{\rho}\bar{\kappa} + a_3\bar{\kappa}^2$+h.o.t. as an approximation for the center manifold, where the bars indicate the new coordinate after translation. After some calculations, we obtain the values $a_1 = 1 + \frac{3}{4}\sqrt{3}, a_2 = 0,$ and $a_3 = 0$ so that $h(\bar{\rho}, \bar{\kappa}) = (1 + \frac{3}{4}\sqrt{3})\bar{\rho}^2$. The following equation gives the flow on the center manifold.

$$\begin{aligned} \bar{\rho}' &= -\bar{\rho}(\bar{\kappa} + 2\bar{\rho} + 2(1 + \frac{3}{4}\sqrt{3})\bar{\rho}^2) \\ \bar{\kappa}' &= 0. \end{aligned} \tag{5.9}$$

We see from the flow (5.9) that we have a super-critical pitchfork bifurcation around (0,0). At $\bar{\kappa} = 0$, the point (0,0) which corresponds with the semi-trivial solution $\mathbf{x_{20}}$ branches off; The semi-trivial solution loses its stability while a stable non-trivial solution is initiated. The non-trivial solution which occurs corresponds with the point $(\frac{2\beta\kappa}{\gamma_1\gamma_2}(1-\frac{3}{4}\frac{\kappa^2}{\gamma_2^2}), -\frac{\kappa}{\gamma_2})$ (or $\mathbf{X_1}$ in ρ–u–v space).

Now we investigate the stability of the non-trivial solution. After substituting $(\frac{2\beta\kappa}{\gamma_1\gamma_2}(1 - \frac{3}{4}\frac{\kappa^2}{\gamma_2^2}), -\frac{\kappa}{\gamma_2})$ into matrix J_2, we obtain the corresponding 2×2 Jacobian matrix.

$$J_h = \begin{pmatrix} 0 & -\frac{2\beta\kappa}{\gamma_1}(1 - \frac{3}{4}\frac{\kappa^2}{\gamma_2^2}) \\ \frac{1}{4}\gamma_1 & \frac{1}{2}\beta(1 - \frac{9}{4}\frac{\kappa^2}{\gamma_2^2}) \end{pmatrix} \tag{5.10}$$

We see from (5.10) that $\kappa = \frac{2}{3}\gamma_2$ is another bifurcation value where the fixed point changes its properties as κ varies. We can check that for $\kappa > \frac{2}{3}\gamma_2$ the corresponding fixed point is a stable focus while for $\kappa < \frac{2}{3}\gamma_2$ the corresponding fixed point is an unstable focus. At the critical value we have a Hopf bifurcation with a pair of purely imaginary eigenvalues. In analyzing the bifurcation, using the center manifold method, we will look for the approximation for the center manifold, the flow in the center manifold, and determine the stability of the limit cycle associated with Hopf bifurcation. First we translate the point $(\frac{2\beta\kappa}{\gamma_1\gamma_2}(1-\frac{3}{4}\frac{\kappa^2}{\gamma_2^2}), -\frac{\kappa}{\gamma_2})$ to $(\hat{\rho}, \hat{v}) = (0, 0)$ and $\kappa = \frac{2}{3}\gamma_2$ to $\hat{\kappa} = 0$, where the hats indicate the corresponding new coordinate after translation. We take the same values of $\beta = 2,\ \gamma_1 = 1,\ \gamma_2 = 2$ as before. To avoid the algebraic complexity due to the presence of the parameter $\hat{\kappa}$, we take $\hat{\kappa} = 0$ from the beginning. Thus, we have the Jacobian matrix of the form

$$A = \begin{pmatrix} 0 & -\frac{32}{9} \\ \frac{1}{4} & 0 \end{pmatrix} \tag{5.11}$$

After normalization and applying the center manifold approach, we obtain the center manifold where the corresponding flow is given by

$$\begin{aligned} \hat{\rho}' &= -\frac{2}{3}\sqrt{2}\hat{v} - 2\hat{\rho}\hat{v} \\ \hat{v}' &= \frac{2}{3}\sqrt{2}\hat{\rho} + \frac{3}{2}\hat{v}^2 - \frac{3}{4}\hat{v}^3. \end{aligned} \tag{5.12}$$

The stability of the limit cycle which occurs can be determined by calculating the following quantity. (See [2] for a formal presentation of the formula).

$$\begin{aligned} a = \frac{1}{16}[f_{xxx} + f_{xyy} + g_{xxy} + g_{yyy}] + \frac{1}{16\omega_0}[f_{xy}(f_{xx} + f_{yy}) \\ - g_{xy}(g_{xx} + g_{yy}) - f_{xx}g_{xx} + f_{yy}g_{yy}], \end{aligned} \tag{5.13}$$

where $\omega_0 = \frac{2}{3}\sqrt{2}$, f, g are, respectively, the right-hand sides of $\hat{\rho}', \hat{v}'$ of (5.12), and the subscripts 'x' and 'y' denote derivation with respect to $\hat{\rho}$ and $\hat{v}$, respectively. We obtain $a = -\frac{9}{32}$, which is negative. Thus, we have a super-critical Hopf bifurcation; a stable limit cycle occurs while the periodic solution changes its stability. To illustrate this phenomenon, we implement the numerical continuation packages CONTENT and DSTOOL, on the basis of the analytical results above. (See [5] for more about the packages).

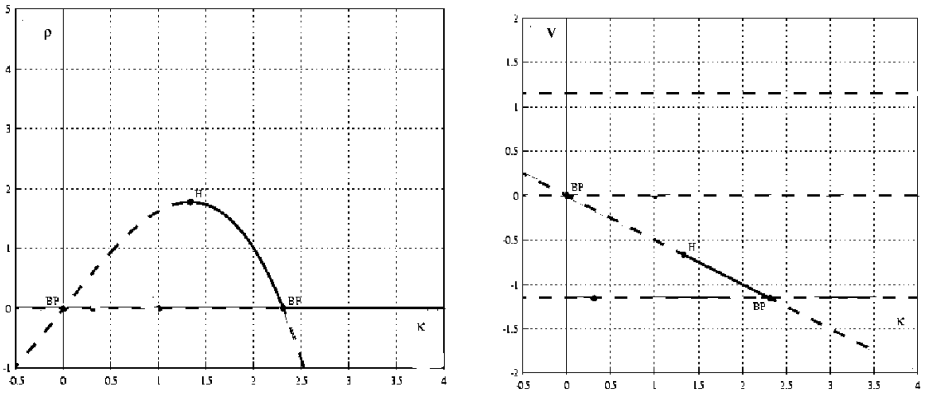

(i) (ii)

Figure 3: **Exact resonance**. Bifurcation diagram of system (5.8) on (i) the $\kappa-\rho$ plane and (ii) the $\kappa-v$ plane, for $\beta = 2$, $\gamma_1 = 1$, $\gamma_2 = 2$. BP stands for branching point and H stands for Hopf point. Solid and dashed lines/curves indicate a stable and an unstable solution, respectively.

Figure 3 gives the corresponding bifurcation diagram which describes the fixed points by giving ρ and v as a function of κ and their stabilities and bifurcations. As commonly used, in bifurcation diagrams displayed in this paper stable solutions are indicated by solid lines/curves and unstable ones by dashed lines/curves. To illustrate the dynamics in the $\rho-v$ plane, especially near the bifurcation point, we refer to Figure 4.

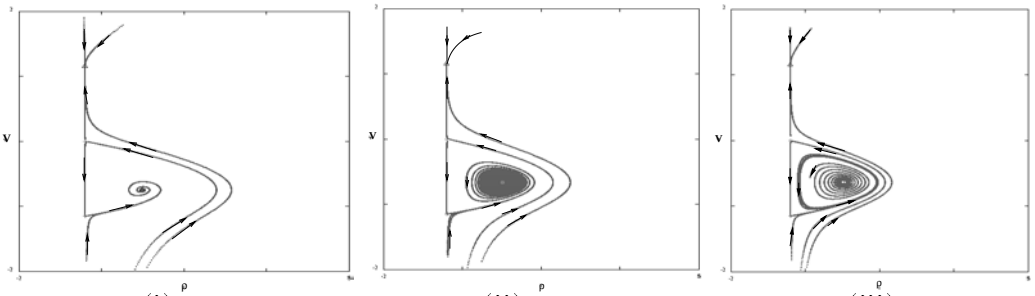

Figure 4: **Hopf bifurcation**. The dynamics in the ρ–v plane for $\beta = 2$, $\gamma_1 = 1$, $\gamma_2 = 2$. (i) at $\kappa = 1.5$, (ii) at $\kappa = \frac{4}{3}$ (the Hopf point), (iii) at $\kappa = 1.28$.

Figure 4 (ii) shows the starting point where the stable limit cycle occurs while the non-trivial solution changes its stability (from a stable focus (in Figure 4 (i)) to an unstable focus (in Figure 4 (iii)).

Continuation with respect to the value of κ on the limit cycle produced by the Hopf bifurcation, results in the stable limit cycle breaking down into a heteroclinic cycle which takes place at $\kappa \approx 1.243761$; The orbit connects the saddle points $(0,0)$ and $(0,-\sqrt{\frac{4}{3}})$ which correspond with the points $\mathbf{x_{00}}$ and $\mathbf{x_{20}}$, respectively. Moreover, perturbing the value of κ by decreasing it, the heteroclinic cycle breaks up. Thus, we have a heteroclinic bifurcation as shown in Figure 5. Figure 5 (i) shows that the stable limit cycle is getting closer to the heteroclinic cycle connecting the saddle points $(0,0)$ and $(0,-\sqrt{\frac{4}{3}})$. Figure 5 (ii) shows that the limit cycle breaks down into a heteroclinic cycle. Finally, in Figure 5 (iii) the heteroclinic cycle breaks up and we have another saddle-sink connection connecting the saddle point $(0,-\sqrt{\frac{4}{3}})$ and the stable node $(0,\sqrt{\frac{4}{3}})$.

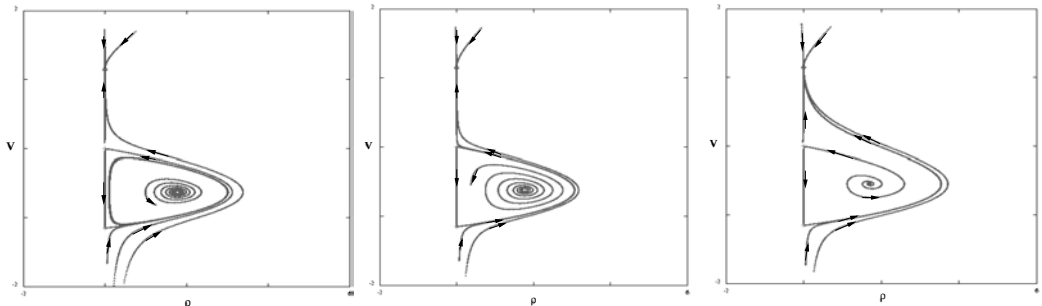

Figure 5: **Heteroclinic bifurcation**. The dynamics in the $\rho - v$ plane for $\beta = 2,\ \gamma_1 = 1,\ \gamma_2 = 2$. (i) at $\kappa = 1.26$, (ii) at $\kappa \approx 1.243761$ (the heteroclinic cycle bifurcation), (iii) at $\kappa = 1.1$.

Continuing to vary the value of κ we find the persistence of the saddle-sink connection.

Now, we analyze the point $\mathbf{X_2}$ which is neither in the u–v plane nor in the $\rho - v$ plane. To apply linear analysis, we substitute the non-trivial solution $\mathbf{X_2}$ (we take the plus sign) into the Jacobian matrix J to obtain the following matrix.

$$\begin{pmatrix} 0 & 0 & -\frac{16}{3}\frac{\gamma_2^2(1-2\frac{\kappa}{\beta})}{\gamma_1} \\ 0 & -\frac{1}{12}\beta\mathcal{C}_2 & (\frac{1}{4}\frac{\beta\kappa}{\gamma_2}+\frac{1}{3}\gamma_2)\sqrt{\mathcal{C}_2} \\ \frac{1}{4}\gamma_1 & (\frac{1}{4}\frac{\beta\kappa}{\gamma_2}-\frac{2}{3}\gamma_2)\sqrt{\mathcal{C}_2} & -\frac{3}{4}\frac{\beta\kappa^2}{\gamma_2^2}+\kappa \end{pmatrix} \tag{5.14}$$

where $\mathcal{C}_2 = 12 - 9\frac{\kappa^2}{\gamma_2^2} - 24\frac{\kappa}{\beta}$. Because of the complexity of the expressions in (5.14) we perform a numerical calculation to obtain the eigenvalues. The eigenvalues of the Jacobian matrix (5.14) are one real and two complex conjugate which are of the form $\mathbf{c}$ and $\mathbf{d} \pm \mathbf{i}\mathbf{e}$. Taking $\mathbf{c} = 0$, which corresponds with taking $\kappa \approx 0.861002$ (for $\gamma_1 = 1,\ \gamma_2 = 2,\ \beta = 2$), the Jacobian has one zero eigenvalue and two complex conjugate eigenvalues. This corresponds with a branching point where the curve of $\mathbf{X_2}$ points parameterized by κ tangents to the curve of $\mathbf{X_1}$ points. Moreover, taking $\mathbf{d} = 0$ which corresponds with $\kappa \approx 0.578051$ (for $\gamma_1 = 1,\ \gamma_2 = 2,\ \beta = 2$), the Jacobian has one real eigenvalue and two purely imaginary eigenvalues. This implies the presence of a sub-critical Hopf bifurcation; an unstable limit cycle occurs while the fixed point changes its stability. Now we have a complete bifurcation

diagram for system (5.1). We describe the fixed points by giving ρ, u, and v as a function of κ as shown in Figure 6.

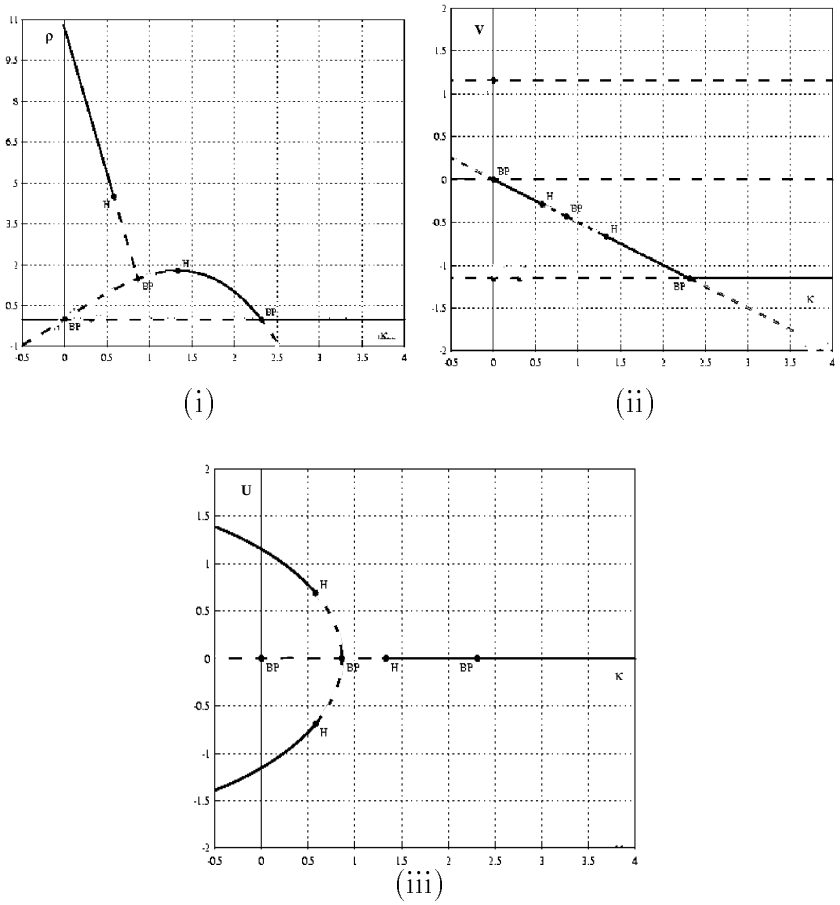

Figure 6: **Exact resonance**. Bifurcation diagram of system (5.1) (i) projected on the $\kappa - \rho$ plane, (ii) projected on the $\kappa - v$ plane, (iii) projected on $\kappa - u$ plane, for $\beta = 2,\ \gamma_1 = 1,\ \gamma_2 = 2$. BP stands for branching point and H stands for Hopf point.

Figure 6(i) and Figure 6(ii) are similar to Figure 3(i) and Figure 3(ii), respectively, except that we have new branches of non-trivial solutions which correspond with $\mathbf{X_2}$. These solutions are shown clearly in Figure 6(iii).

5.2 The heteroclinic cycle

By combining the dynamics in the $u-v$ plane (see Figure 2) and Figure 5 (iii) we obtain a *robust heteroclinic cycle*; a cycle which is formed by two saddle-sink connections of the invariant manifolds $u-v$ plane and $\rho-v$ plane. (See [3] for the definition). This, actually, also follows from system (5.1) when we integrate a point nearby the unstable non-trivial solution for $\kappa < 1.243761$. Figure 7 gives a clear illustration of the cycle in the 3-dimensional phase-space $\rho-u-v$.

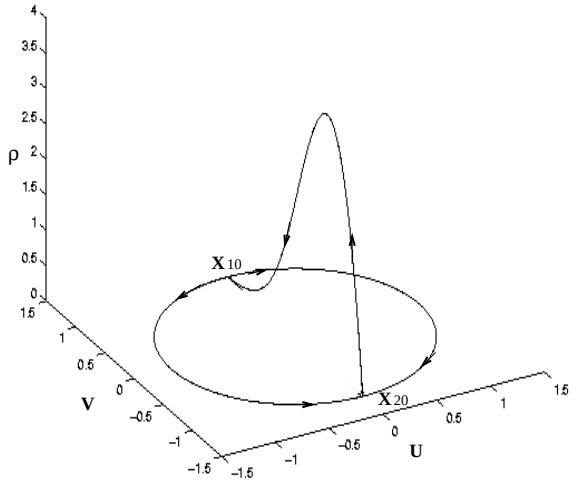

Figure 7: The robust heteroclinic cycle connecting the saddle points $\mathbf{x_{10}}$ and $\mathbf{x_{20}}$.

In the original system (4.3), $\mathbf{x_{10}}$ and $\mathbf{x_{20}}$ should be identified and correspond with the semi-trivial periodic solution. In system (4.3) the part of the heteroclinic cycle for $\rho > 0$ corresponds with a solution homoclinic to the semi-trivial periodic solution.

Note that since the heteroclinic cycle persists in the interval of κ where no stable solution takes place (see the bifurcation diagram of Figure 3), we may further the analysis by studying the stability of the heteroclinic cycle.

Studies on the stability of robust heteroclinic cycles have been done by several authors. (See, for example, [3], [4], and the references there). In [4] Krupa and Melbourne develop a general sufficient and necessary condition for investigating the asymptotic stability of such cycles. They use the fact

that a trajectory following the robust heteroclinic cycle (see Figure 7) will spend large amounts of time near the fixed points ($\mathbf{x_{10}}$ and $\mathbf{x_{20}}$) while the passages outside fixed points will be relatively short. Hence the relative size of the eigenvalues of the linearizations at the fixed points will be the factor determining stability. The discussion below will follow this idea.

First, we take the same fixed values of the parameters $\beta = 2,\ \gamma_1 = 1,\ \gamma_2 = 2$ as before and assume that we are in the interval of κ where we have unstable solutions only. So, we may take $\kappa = 1$. Recall that the point $\mathbf{x_{10}}$ is a saddle point with its stable eigenvalues $\lambda_{s_1} = -1 - 2\sqrt{\frac{4}{3}}$ and $\lambda_{s_2} = -2$ are in the $\rho - v$ plane, while the unstable one $\lambda_u = 2\sqrt{\frac{4}{3}}$ is in the $u - v$ plane. The point $\mathbf{x_{20}}$ is a saddle point with its stable eigenvalues $\nu_{s_1} = -2\sqrt{\frac{4}{3}}$ and $\nu_{s_2} = -2$ are in the $u - v$ plane while its unstable eigenvalue $\nu_u = -1 + 2\sqrt{\frac{4}{3}}$ is in the $\rho - v$ plane. Thus, our heteroclinic cycle is formed by two saddle-sink connections as obtained earlier. This is clear from Figure 7 above.

Then we implement the result in [4] saying that if S is a robust heteroclinic cycle then S is asymptotically stable provided the condition

$$\prod_{j=1}^{m} \min(c_j, e_j - t_j) > \prod_{j=1}^{m} e_j, \tag{5.15}$$

is satisfied, where

- c_j is the magnitude of the maximal real part of the eigenvalue of $Df(\xi_j)$, linearized vector field near fixed point, restricted to $P_{j-1} \backslash P_j$,
- e_j is the magnitude of the maximal real part of the eigenvalue of $Df(\xi_j)$ restricted to $P_j \backslash P_{j-1}$,
- t_j is the maximal real part of the eigenvalues whose eigenvectors are normal to $P_{j-1} + P_j$,

with $P_{j-1},\ P_j$ the corresponding invariant subspaces. (See Theorem 2.7 of [4] for more detail in the formulation). We change the condition (5.15) slightly since in our case, we do not have t_j. Therefore condition (5.15) reduces to the standard condition that

$$\prod_{j=1}^{m} c_j > \prod_{j=1}^{m} e_j. \tag{5.16}$$

From the eigenvalues of $\mathbf{x_{10}}$ and $\mathbf{x_{20}}$ mentioned above we obtain that $\frac{\lambda_{s_1}\nu_{s_1}}{\lambda_u\nu_u} \approx 1.322781 > 1$. Thus, by (5.16) we conclude that our heteroclinic cycle is asymptotically stable. Therefore, this gives the boundedness of the solution in the interval of the parameter κ where no stable periodic solution takes place.

We find that the stable heteroclinic cycle persists as we vary the value of κ. This is due to the persistence of the corresponding saddle-sink connections mentioned earlier. Thus, in the interval $0 < \kappa < 0.578051$ we have two attractors; the stable heteroclinic cycles and the stable fixed points produced by the sub-critical Hopf bifurcation (see the analysis of the point $\mathbf{X_2}$ mentioned earlier). Therefore, the dynamics in that region is attracted either to the fixed point $\mathbf{X_2}$ or to the heteroclinic cycle.

6 Near-resonance

In this section we analyze the full averaged system (4.5) by considering $\sigma \neq 0$. In system (4.5) the symmetry $(\rho,\ u,\ v) \to (\rho,\ -u,\ v)$ which takes place in the exact resonance case no longer exists while we keep the invariance of $\rho = 0$. In the following we discuss this symmetry breaking property when σ is perturbed from 0 as it reflects on the solutions, stabilities and bifurcations, as κ varies.

We follow similar lines for determining fixed points as in the previous section, and obtain the following fixed points. $\mathbf{y_{00}} = (\rho_1, u_1, v_1) = (0,0,0)$ (the trivial solution), $\mathbf{y_{10}} = (0, -\frac{2\sigma}{\gamma_2}, \sqrt{\frac{4}{3} - \frac{4\sigma^2}{\gamma_2^2}})$, and $\mathbf{y_{20}} = (0, -\frac{2\sigma}{\gamma_2}, -\sqrt{\frac{4}{3} - \frac{4\sigma^2}{\gamma_2^2}})$ (the semi-trivial solution), and the non-trivial solutions

$$\mathbf{Y_1} = (\rho_1(u_1), u_1, -\frac{\kappa}{\gamma_2}), \tag{6.1}$$

where u_1 will be determined from the following cubic polynomial in u_1.

$$u_1^3 + (\frac{3\beta\kappa^2 + 8\kappa\gamma_2^2 - 4\beta\gamma_2^2}{3\beta\gamma_2^2})u_1 + \frac{16}{3}\frac{\kappa\sigma}{\beta\gamma_2} = 0 \tag{6.2}$$

Using Cardano's formula for solving a cubic equation, we determine the quantity $\mathcal{D} = \frac{q^2}{4} + \frac{p^3}{27}$, where $p = \frac{16}{3}\frac{\kappa\sigma}{\beta\gamma_2}$, $q = \frac{3\beta\kappa^2 + 8\kappa\gamma_2^2 - 4\beta\gamma_2^2}{3\beta\gamma_2^2}$. After a rather lengthy calculation we arrive to the following expression for $\mathcal{D}$.

$$\mathcal{D} = \frac{1}{729\beta^3\gamma_2^6}((\beta - \beta_0)^3 + 5184\beta\gamma_2^4\kappa^2\sigma^2), \tag{6.3}$$

where

$$\beta_0 = \frac{8\gamma_2^2\kappa}{4\gamma_2^2 - 3\kappa^2}. \tag{6.4}$$

From (6.4) we restrict the value of κ into $0 < \kappa < \gamma_2\sqrt{\frac{4}{3}}$. Then, Cardano's formula guarantees the existence of at least one real solution for u_1 in (6.2) which unfortunately has a quite complicated expression.

Next, we analyze the stability of the fixed points by using the same method as before. We consider the Jacobian matrix of system (4.5) as follows.

$$J_s = \begin{pmatrix} -\kappa - \gamma_2 v & 0 & -\gamma_2 r \\ 0 & \frac{1}{2}\beta - \frac{9}{8}\beta u^2 - \frac{3}{8}\beta v^2 + \gamma_2 v & -\frac{3}{4}\beta uv + \gamma_2 u + 2\sigma \\ \frac{1}{4}\gamma_1 & -\frac{3}{4}\beta uv - 2\gamma_2 u - 2\sigma & \frac{1}{2}\beta - \frac{3}{8}\beta u^2 - \frac{9}{8}\beta v^2 \end{pmatrix} \tag{6.5}$$

Since the plane $\rho = 0$ is an invariant manifold we start the analysis from the points in that plane, i.e. $(0,0)$, $(-\frac{2\sigma}{\gamma_2}, \sqrt{\frac{4}{3} - \frac{4\sigma^2}{\gamma_2^2}})$, and $(-\frac{2\sigma}{\gamma_2}, \sqrt{\frac{4}{3} - \frac{4\sigma^2}{\gamma_2^2}})$ which correspond to $\mathbf{y_{00}}$, $\mathbf{y_{10}}$, and $\mathbf{y_{20}}$, respectively. Linear analysis gives the results that the point $(0,0)$ is an unstable focus, $(-\frac{2\sigma}{\gamma_2}, \sqrt{\frac{4}{3} - \frac{4\sigma^2}{\gamma_2^2}})$ is a saddle, and $(-\frac{2\sigma}{\gamma_2}, -\sqrt{\frac{4}{3} - \frac{4\sigma^2}{\gamma_2^2}})$ is a stable node as shown in the following figure.

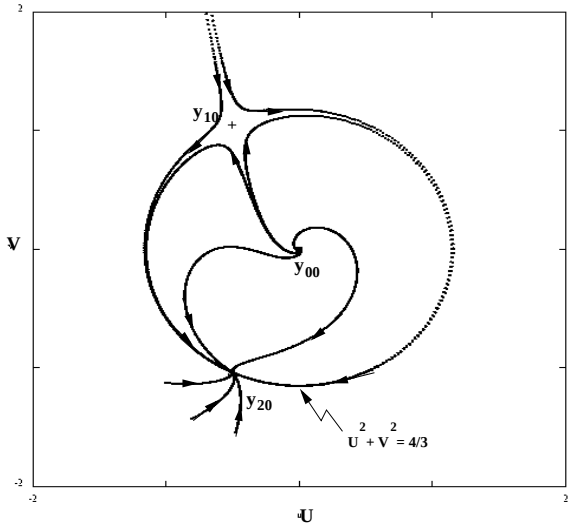

Figure 8: The dynamics in the $u-v$ plane for $\sigma = 0.5$

If we compare Figure 8 with Figure 2, points $\mathbf{y_{00}}$, $\mathbf{y_{10}}$, and $\mathbf{y_{20}}$ actually correspond with points $\mathbf{x_{00}}$, $\mathbf{x_{10}}$, and $\mathbf{x_{20}}$, respectively. Those Figures show that the σ perturbation does not change qualitatively the dynamics in the $u-v$ plane. Also, in the $u-v$ plane we have a separatrix $u^2+v^2=\frac{4}{3}$ which corresponds with the semi-trivial solution. Then, the semi-trivial solution will bifurcate for a certain value of κ where the non-trivial solution $\mathbf{Y_1}$ is initiated.

Due to the complexity of the expression of $\mathbf{Y_1}$ we perform numerical approaches to determine its stability. Solving Det $J_s\Big|_{\mathbf{Y_1}}=0$, we obtain a parameter space $\kappa-\sigma$ showing the stability boundary for the solutions where the stable semi-trivial solution passing through the boundary branches off in a pitchfork bifurcation. This is shown by curve P in Figure 9. Furthermore, continuation by using CONTENT we obtain a Hopf curve H in Figure 9 where the non-trivial solutions have Hopf bifurcations and a saddle-node curve SN in Figure 9 where the non-trivial solutions have saddle-node bifurcations.

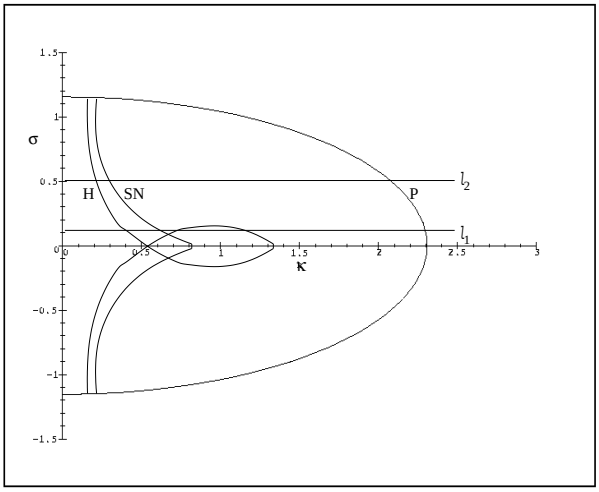

Figure 9: **Near resonance**. The parameter space $\kappa-\sigma$ showing Curves P, H, and SN for $\beta=2,\ \gamma_1=1,\ \gamma_2=2$.

Note that the boundedness of the range of σ is clear from the existence of the above mentioned semi-trivial solution, $\mathbf{y_{10}}$ and $\mathbf{y_{20}}$. Figure 10 and Figure 11 are the corresponding bifurcation diagrams which describe the number of solutions and their stabilities and bifurcations by giving ρ and u as a function of κ.

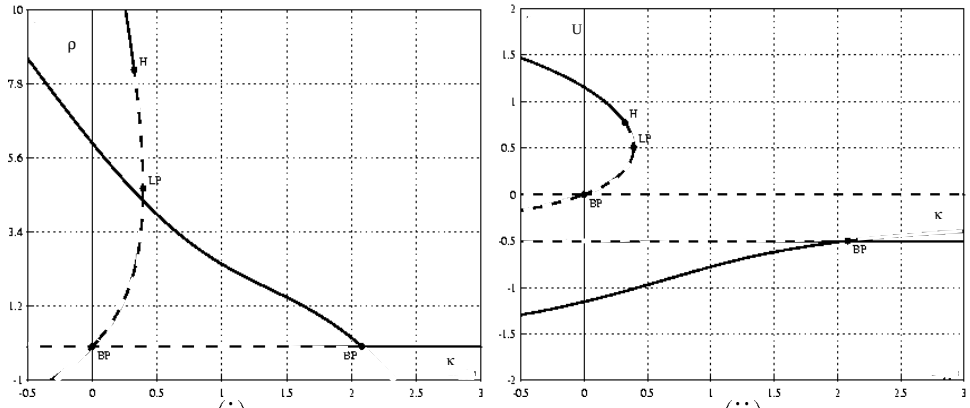

(i) (ii)

Figure 10: **Near resonance**. Bifurcation diagram of system (4.5) (i) projected on the $\kappa - \rho$ plane and (ii) projected on the $\kappa - u$ plane, for $\beta = 2,\ \gamma_1 = 1,\ \gamma_2 = 2,\ \sigma = 0.5$ (line l_2). BP stands for pitchfork point, H for Hopf point, and LP for saddle-node point.

Figure 10 (i) and (ii) clearly illustrate the behaviour of the non-trivial periodic solutions of system (4.5) for $\sigma = 0.5$ (line l_2 of Figure 9). We start from the stable semi-trivial solution in the outer part of curve P. As the solution passes through curve P, a pitchfork bifurcation takes place (shown by the BP point on the right); the semi-trivial solution loses its stability while a stable non-trivial solution is initiated. On the other hand, continuation on the unstable trivial solution $\mathbf{y_{00}}$, from the BP point on the left, we obtain an unstable non-trivial solution which undergoes a saddle-node bifurcation (at the LP point) when hitting curve SN. Then, the unstable non-trivial solution undergoes a sub-critical Hopf bifurcation (at the H point) when passing through curve H.

It is interesting to see what happens to the non-trivial solution if we take σ closer to 0. Taking $\sigma = 0.1$ (line l_1 of Figure 9) we have the bifurcation diagram as shown in Figure 11.

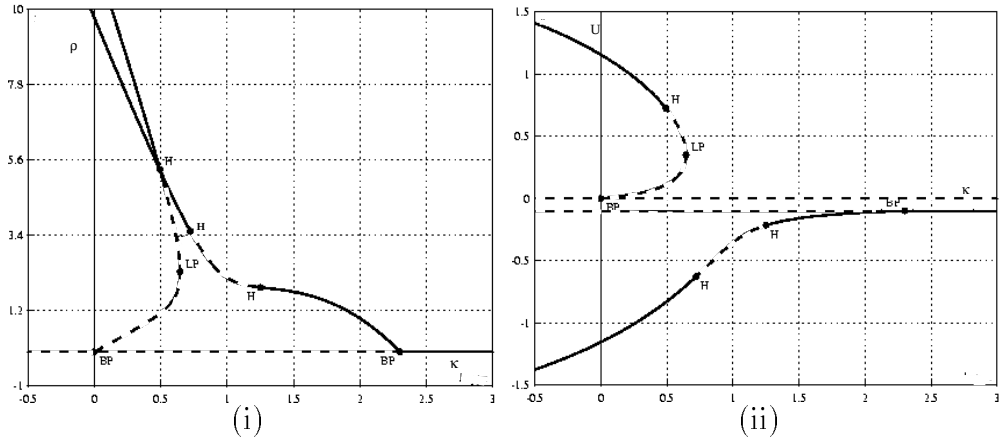

Figure 11: **Near resonance**. Bifurcation diagram of system (4.5) (i) projected on the $\kappa - \rho$ plane and (ii) projected on the $\kappa - u$ plane, for $\beta = 2,\ \gamma_1 = 1,\ \gamma_2 = 2,\ \sigma = 0.1$ (line l_1). BP stands for pitchfork point, H for Hopf point, and LP for saddle-node point.

Figure 11 shows more complicated dynamics than Figure 10. Obviously, Figure 11 (i) and (ii) tend to, respectively, Figure 6 (i) and (iii) of the exact resonance case if we take σ closer to 0. However, taking $\sigma \neq 0$ means we slightly perturb equation (5.1) such that the symmetry under $u = 0$ is broken; a *forced symmetry breaking* takes place. (See Krupa [3]). Thus, destruction of the stable robust heteroclinic orbit obtained earlier will take place. In [10] Swift shows that forced symmetry breaking for such an attracting orbit leads to the occurrence of a long-periodic orbit. We perform a numerical exploration to demonstrate the phenomenon in our system.

Taking an initial point nearby the robust heteroclinic orbit, it will go to a"one-half" orbit which has a long-period as shown in Figure 12 (i) and (ii) depending on the sign of σ. And Figure 12 (iii) gives a clear illustration of the forced symmetry breaking phenomenon if we compare it with Figure 7 of the exact resonance case.

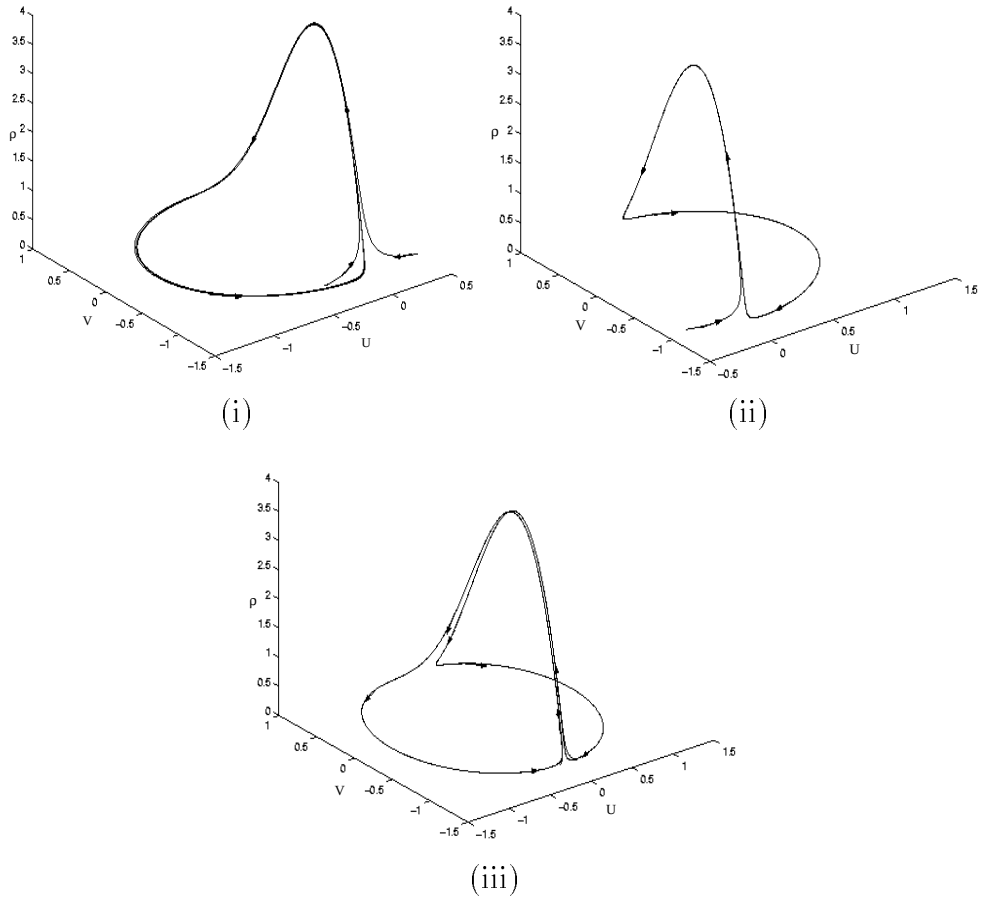

Figure 12: **Forced symmetry breaking**. (i) a long-periodic orbit for $\sigma = 0.01$, (ii) a long-periodic orbit for $\sigma = -0.01$, (iii) the combination of (i) and (ii).

7 Concluding remarks

The study of stability and bifurcation of the solutions of system (2.1) produces rich results as we have shown in the previous sections. Our results on the stability of the semi-trivial solution of such a system plays an important role in mechanical engineering. The exact resonance analysis gives interesting phenomena, especially the boundedness of the solution shown by the attracting robust heteroclinic orbit. More interesting and important results

are obtained from the near resonance analysis. We have shown numerically what happens with the solutions of our system if we apply the detuning coefficient.

A study of self-excited auto-parametric systems of different type (e.g. van der Pol type) is also of interest. In our future work we will explore that type of system (see the work of Nabergoj and Tondl in [6] or Tondl et al. in [13]) and we will compare the results to those of this paper. Of course we can generalize system (2.1), for instance by generalizing the coupling term. The result of this have to be studied but we expect to recover the fundamental bifurcations discussed in this paper.

Acknowledgments. The author would especially like to thank Prof. dr. Ferdinand Verhulst for the support, encouragement and inspiration which he offered during the preparation of this paper. The author would like to thank Prof. Aleš Tondl for helping in formulating the problems of this paper. Many thanks to Yuri A. Kuznetsov, Ale Jan Homburg, Siti Fatimah and Theo Tuwankotta, for the inspiring and encouraging discussions. Finally, the author's special thanks to the author's family in Indonesia for their support and patience.

References

[1] Carr, J., *Applications of Centre Manifold Theory*, Appl.Math.Sciences 35, Springer-Verlag, New York, 1981.

[2] Guckenheimer, J. and Holmes, P., *Nonlinear Oscillations, Dynamical Systems, and Bifurcations of Vector Fields*, Appl.Math.Sciences 42, Springer-Verlag, New York, 1997.

[3] Krupa, M., Robust Heteroclinic Cycles, *J. Nonlinear Sci.* 7, 1997, 129-176.

[4] Krupa, M. and Melbourne, I., Asymptotic Stability of Heteroclinic Cycles in Systems with Symmetry, *Ergod. Th. & Dynam. Sys.* 15, 1995, 121-147.

[5] Kuznetsov, Y. A., *Elements of Applied Bifurcation Theory*, Appl.Math.Sciences 112, Springer-Verlag, New York, 1998.

[6] Nabergoj, R. and Tondl, A., Autoparametric Resonance in Self-Excited Single Mass System, in *Proceedings of the EUROMECH-2nd European Nonlinear Oscillation Conference*, Prague, Sep. 9-13, 1996, 151-156.

[7] Ruijgrok, M., *Studies in Parametric and Autoparametric Resonance*, Thesis, Utrecht University, 1995.

[8] Schmidt, G. and Tondl, A., *Non-linear Vibrations*, Cambridge University Press, Cambridge, 1986.

[9] Sanders, J. A. and Verhulst, F., *Averaging Methods in Nonlinear Dynamical Systems*, Appl. Math. Sciences 59, Springer-Verlag, New York, 1985.

[10] Swift, J. W., Convection in a Rotating Fluid Layer, *Contemporary Mathematics* 28, AMS, 1984, 435-448.

[11] Tondl, A., *Quenching of Self-Excited Vibrations*, Elsevier, Prague, 1991.

[12] Tondl, A. and Nabergoj, R., *Autoparametric Systems* , Report No. 16, Department of Naval Architecture, Ocean and Environmental Engineering, Trieste, 1993.

[13] Tondl, A. et al., *Autoparametric Resonance in Mechanical Systems*, Cambridge University Press, New York, 2000.

[14] Verhulst, F., *Nonlinear Differential Equations and Dynamical Systems*, Springer-Verlag, Berlin, 1996.

[15] Wiggins, S., *Introduction to Applied Nonlinear Dynamical Systems and Chaos*, Springer-Verlag, New York, 1990.